Tectonophysics 510 (2011) 172–185

Contents lists available at ScienceDirect

Tectonophysics

journal homepage: www.elsevier.com/locate/tecto

Crustal inhomogeneities in the Northern North Sea from potential field modeling: Inherited structure and serpentinites?

Christine Fichler [a,*], Tore Odinsen [b], Håkon Rueslåtten [c], Odleiv Olesen [d], Jens Emil Vindstad [a], Susann Wienecke [a]

[a] Statoil ASA, NO-7005 Trondheim, Norway
[b] Statoil ASA, Sandslihaugen 30, NO-5254 Sandsli, Norway
[c] Numerical Rocks AS, NO-7041 Trondheim, Norway
[d] Geological Survey of Norway, Postboks 6315 Sluppen, NO-7491 Trondheim, Norway

ARTICLE INFO

Article history:
Received 12 October 2010
Received in revised form 23 June 2011
Accepted 30 June 2011
Available online 13 July 2011

Keywords:
Viking Graben
Gravity anomaly
Magnetic anomaly
Serpentinites
Meta-peridotites
Lower crustal body

ABSTRACT

A new crustal model for the northern North Sea was developed by gravity and magnetic modeling along the deep seismic line NSDP84-1. Utilizing vertical gradients allowed distinguishing between shallow and deep crustal sources. The upper crust is characterized by low magnetic susceptibilities and low densities, which is typical for felsic rocks. A new finding was that the deep crust below the western Viking Graben and the East Shetland Basin is the source of high magnetic anomalies combined with low gravity anomalies, which was interpreted to represent rocks with very high magnetic susceptibilities and low to intermediate densities. Such rock parameters may indicate serpentinites, but intermediate intrusives or a combination of both is also possible. Honoring the string of three near equidistant magnetic maxima, which follow the trend of the NNE–SSW striking East Shetland Basin in the map plane, it is suggested that this area is part of an island arc of the Iapetus Ocean which has been assembled during the collision between Laurentia and Baltica in late Silurian times. Partly serpentinized peridotites and intermediate intrusives will relate in such a model to slab dehydration of the subducting oceanic plate below the island arc. These inherited or synorogenic serpentinites are expected to persist in the geothermal regime of the Caledonian orogeny to a depth of at least 50 km. Increased heat flow by later rift phases will have caused metamorphism of the remaining serpentinites to meta-peridotites at depth below the present day Moho. Fluid release related to dehydration of the serpentinites may have triggered further serpentinization of the inherited, partly serpentinized rocks at shallower depth. An alternative origin for the suggested serpentinites, valid only for the area under the western part of the Viking Graben, may be synrift serpentinization due to the heavy faulting during the Jurassic rift phase.

1. Introduction

The northern North Sea is one of the world's best explored and understood sedimentary basins, as it hosts hydrocarbon source rocks and reservoirs. Its sedimentary stratigraphy has been mapped to a high degree of accuracy by reflection seismic data and wells (e.g., Evans et al., 2003; Glennie, 1990). However, the sedimentary history starts as "young" as in the Devonian with the deposition of sediments on the crystalline basement. The underlying crust, the focus of this study, consists of rocks formed during a much longer period which includes at least one Wilson cycle with the opening of the Iapetus Ocean, island arc development connected to oceanic subduction, suture and Caledonian orogeny (e.g., Fossen et al., 2008). These processes have been investigated in great detail onshore Norway (e.g., Ramberg et al., 2008). However, offshore basement knowledge is rather scarce, due to limited basement well control. This forces the crustal model to be built from interpretation of geophysical data and extrapolation of geological knowledge from the surrounding land areas.

We revisited the deep seismic line NSDP84-1 (Fig. 1). This line has earlier been modeled with gravity data (Fichler and Hospers, 1990a,b; Holliger and Klemperer, 1989) and later reprocessing of these data has indicated a high velocity, high density lower crustal body (LCB) under the Horda Platform (Christiansson et al., 2000). Now, we included magnetic data as well as vertical gradients of gravity and magnetic data which allowed a more specific interpretation in terms of basement petrology as well as distinction between upper and lower crustal structure. We further included recently published dating of basement well cores.

* Corresponding author. Tel.: +47 90959351.
E-mail addresses: chrif@statoil.com (C. Fichler), todin@statoil.com (T. Odinsen), haakon@numericalrocks.com (H. Rueslåtten), Odleiv.Olesen@ngu.no (O. Olesen), jevi@statoil.com (J.E. Vindstad), suw@statoil.com (S. Wienecke).

0040-1951/$ – see front matter © 2011 Elsevier B.V. All rights reserved.
doi:10.1016/j.tecto.2011.06.026

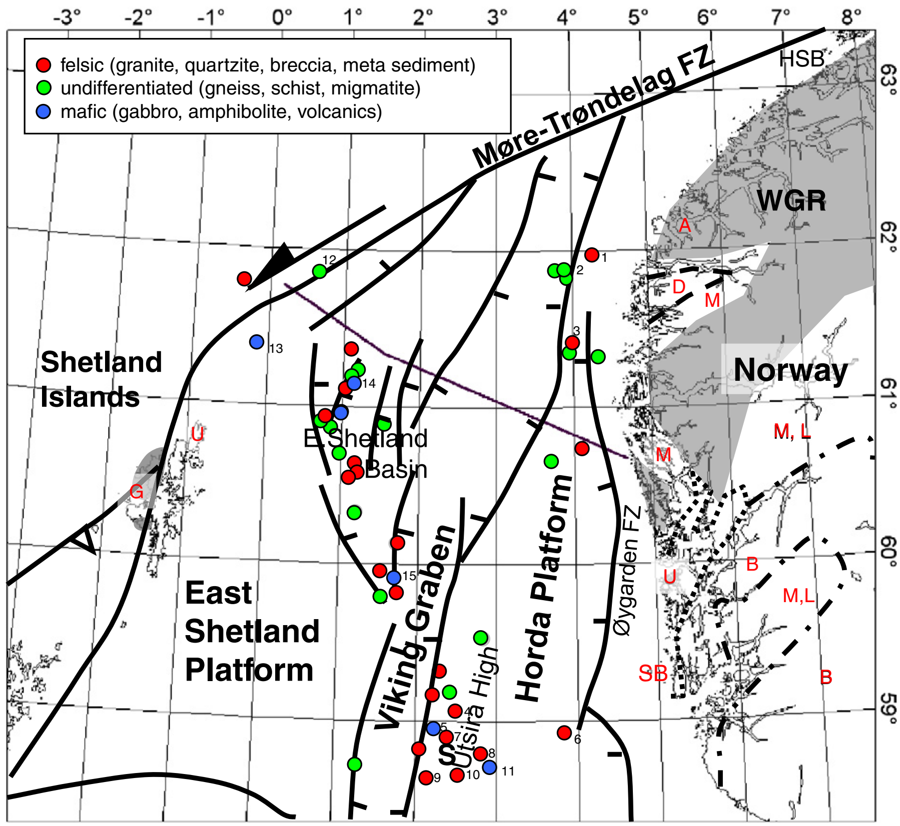

Fig. 1. Tectonic framework of the northern North Sea (Coward, 1990; Gabrielsen et al., 1999; Zanella and Coward, 2003). The thin line shows the location of the interpreted part of the deep seismic line NSDP84-1. Classified offshore basement well cores refer to Bassett (2003), Olesen et al. (2007) and Slagstad et al. (2011), more information exists on the numbered wells gathered in Table 1. Norway onshore tectonostratigraphical map elements (Fossen et al., 2008): Devonian Basins (D), Upper Allochthon (U), Middle Allochthon (M, basement sheets, sparagmite nappes) and Lower Allochthon (L, sparagmite nappes), Western Gneiss Region (WGR), Basement (B, autochthonous), Almklødvalen ultramafic body (A), Hitra-Smøla-Batholith (HSB), Sunnhordland Batholith (SB). Shetland Islands rocks (Bassett, 2003): Unst-Fetlar Ophiolite (U), Granites (G).

In our study, we focused especially on serpentinites and meta-peridotites. Serpentinites have gained increased scientific interest during the last decade. Appreciable amounts of serpentinites have been proven to exist in different tectonic settings. We shall discuss what kind of serpentinites could have been generated and/or inherited in the North Sea crust.

2. Basement history

The northern North Sea is located within the area of the junction between the Laurentian and Baltican plates, both of which have a long history over more than one Wilson cycle (Bassett, 2003; Glennie, 1990; Livermore et al., 1985; Meert and Torsvik, 2003; Pickering and Smith, 1995). The eastward onshore continuation of the northern North Sea is known as the Western Gneiss Region (WGR; Fig. 1), which is the westernmost part of the Fennoscandian basement of Baltica. We shall resume its extensively investigated and highly complex history utilizing Nordgulen and Andresen (2008) and references herein. Dating of the WGR rocks has revealed its origin and tectonic activity through several Wilson cycles. The oldest rocks are mantle peridotites of apparently Archean protoliths (Spengler et al., 2006). The majority of the rocks were formed in meso- and neo-Proterozoic ages (Tucker et al., 2004), which includes the late Svecofennian—as well as Sveconorwegian period (Rohr et al., 2004). The opening of Rodinia forming the Iapetus Ocean started with a major rift system, at 600–550 Ma, with its axis assumed in the same area and same direction as the North Sea Rift (Meert and Torsvik, 2003). The Iapetus Ocean hosted at least two island arc chains assembled at the western boundary of the Baltican continent. The subsequent Scandian orogeny formed napes, which include parts of the island arcs. Their onshore occurrence has been proven in the Norwegian Bindal-, the Smøla-Hitra- and the Sunnhordland batholiths (Fig. 1; Fossen et al., 2008 and references herein).

During the Scandian orogenic phase, the WGR was buried to depths of up to 150 km. This was followed by a rapid exhumation of the deep crustal root, which we see exposed in the WGR (e.g., Andersen et al., 1991). These processes resulted in a metamorphic overprint of the Proterozoic crust with a progressive increase in pressure and temperature toward the northwest, and with maximum temperatures of 800 °C observed in the area north of Stad, western-most WGR (62°N, 5°E; Dewey et al., 1993).

The southwestern boundary of the northern North Sea shows outcrops of the Laurentian plate on the Shetland Islands (e.g., Cocks and Torsvik, 2003), strongly affected by the Caledonian orogeny. Especially noted is the Unst-Fetlar Ophiolite Complex obducted in late Ordovician (Bassett, 2003, and references herein) as well as granites of Caledonian synorogenic age, as the Skaw granite (Atherton and Ghani, 2002).

The remnants of the rocks which have been involved in the collision and Caledonian orogeny, formed the protolith of the present day North Sea crust. It is anticipated that this protolith with its structures influenced later structural reconfiguration in the area (Færseth et al., 1995; Frost, 1987; Gabrielsen et al., 2010; Hurich and Kristoffersen, 1988; Klemperer and Hurich, 1990). The North Sea crust was strongly affected by two distinct rift phases that post-date the Caledonian extensional collapse. (1) The oldest has been recognized as the Permian—early Triassic rift phase, although both timing and significance have been debated (Færseth et al., 1995; Gabrielsen and Kløvjan, 1990; Giltner, 1987; Odinsen et al., 2000; Roberts et al., 1995). (2) The youngest and best known rifting phase occurred during mid-Jurassic—early Cretaceous times (Eynon, 1981; Færseth, 1996; Gabrielsen and Kløvjan, 1990). Both rift phases have been characterized by regional, E–W to NNW–SSE oriented extension associated with normal faulting and syn-rift sedimentation (e.g., Færseth et al., 1995), and followed by thermal cooling and sediment loading (e.g., Giltner, 1987; Gabrielsen et al., 1990; Roberts et al., 1995).

3. Basement petrology

Direct offshore crustal basement mapping is restricted to a limited number of exploration wells which are compiled in Fig. 1. Petrology analysis, age dating as well as the measurement of geophysical parameters has been performed on some of the well cores (Bassett, 2003, Olesen et al., 2007; Slagstad et al., 2008, 2011; Table 1). Granites, gneisses and meta-sediments are the most dominating rocks. Already in 1982, Donato and Tully have suggested such batholitic type of rocks on the western shoulder of the Viking Graben from gravity modeling, which has later been confirmed by well data (Bassett, 2003). Amphibolites are penetrated by two wells on the northern East Shetland Basin.

The bedrocks in wells 35/3-4 and 36/1-1 ("2" and "1", respectively; Fig. 1, Table 1), are described as gneisses of mesoproterozoic ages (Olesen et al., 2007), similar to onshore rocks of the WGR (Nordgulen and Andresen, 2008). Consequently, an offshore extension of the WGR is supported by these data. The question of the westward extension of the WGR has also been addressed by magnetic mapping. Smethurst (2000) has shown that the onshore magnetic anomalies of the WGR could be followed westward across the N–S striking Øygarden Fault Zone (Fig. 1). Top basement is rapidly deepening from here toward the west (Ebbing and Olesen, 2010; Hospers and Ediriweera, 1988), where the magnetic anomalies fade away by decrease in amplitude and increase in wavelengths (Fig. 2). West of the Øygarden Fault Zone, in the deeper part of the basin, the basement interpretation is restricted to geophysical mapping until shallower basement is reached and well control exists in the East Shetland Basin (Fig. 1).

In the 1990s, a breakthrough has been achieved by interpretation of deep seismic profiles and a first model of the northern North Sea rift structure has been established (Beach, 1986; Gibbs, 1987; Hurich and Kristoffersen, 1988; Klemperer, 1988). Already at that stage, large crustal heterogeneities have been indicated by crustal reflectivity patterns. The next progress has to be attributed to gravity modeling, which has been performed along some of the deep seismic lines (Fichler and Hospers, 1990a, b; Holliger and Klemperer, 1989; Holliger and Klemperer, 1990). The gravity modeling has been performed with a homogeneous crustal density and has indicated crustal thinning to more than one third of the original thickness. This is generally more than what has been estimated from structural modeling or restoration of fault heaves (Gabrielsen et al., 1999; Odinsen et al., 2000; Roberts et al. 1995). Christiansson et al. (2000) detected a large lower crustal body with high velocities and high densities und the Horda Platform (Fig. 3). Christiansson et al. (2000) have suggested this body to partially consist of eclogites similar to – and of the same origin as – the ultra-high pressure metamorphic rocks of the adjacent WGR.

A new result of major and minor element chemistry south of our study area, on the Utsira High, has shown batholiths of oceanic island arc origin, dated as Silurian, prior to the closure of the Iapetus Ocean (Olesen et al., 2007; Bassett, 2003; Slagstad et al., 2011; "5"–"11" in Fig. 1 and Table 1). Similar rock types, also classified as island arc granitoids and dated as coeval with Iapetus oceanic times have also been found onshore southern Norway, which include the Sunnhordland and the Hitra-Smøla batholiths (Fig. 1; Fossen et al., 2008; Slagstad et al., 2011). The volume of island arcs can be estimated from present day island arcs in the western Pacific Ocean. The width of island arcs is typically between 50 and 300 km, and its chains can have a length of several thousands of km (e.g., Winter, 2009). We may therefore expect that island arc rocks are present in the collision zone between Baltica and Laurentia and as such also in the area of the northern North Sea. As a consequence, we can also expect that the lithospheric parts of island arcs, including its oceanic subduction wedges, which typically contain serpentinites, are assembled in the deep crust and lithosphere of the North Sea. The geophysical modeling in the next section was performed with the aim to classify the crustal rocks of northern North Sea and to gain further insight into the tectonic history.

4. Gravity and magnetic modeling

The geophysical data included gravity, magnetic and deep seismic data. The gravity data constitute satellite data, reprocessed by GETECH (Fairhead et al., 2001; Fig. 2). The grid accuracy of these data is estimated to 3 mGal. The magnetic data are referenced to the compilation of Verhoef et al. (1996) and Olesen et al. (2010), shown in Fig. 2. The grid accuracy is estimated to 5 nT. In order to facilitate the distinction between shallow and deep crustal sources, the vertical gradients of the observed gravity and magnetic fields were included in the modeling. These gradients were calculated from the observed map data utilizing the Fourier Transform (e.g., Dobrin and Savit, 1988). The vertical gradient is a high pass filter and enhances as such the short wavelengths, which are related to the shallow sources (cf., Dobrin and Savit, 1988). However, high pass filtering also increases the noise level, which resulted in a rather noisy vertical gradient of the gravity

Table 1
Rock parameters of analyzed well cores, the reference numbers (Ref.) are found in Fig. 1. The letter after the reference number indicates the source; a—Bassett (2003), b—Slagstad et al. (2008), c—Slagstad et al. (2011).

Ref.	Well	Country	Lithology	Geochronologic age (Ma)	Susceptibility [10^{-6}Si]	Remanence (10^{-3} Am^{-1})	Density [g/cm^3]
1b	36/1-1	N	Granitic gneiss		104	5.2	2.676
2b	35/3-4	N	Biotite gneiss		234	0	2.773
3b	35/9-1	N	Breccia		286	0	2.619
4b	25/11-17	N	Metasiltstone		292	0	2.656
5bc	16/1-4	N	Leucogabbro	421	448.4	32.1	2.765
6b	17/3-1	N	Breccia		300	5	2.71
7a	16/2-1	N	Biotite microgranite	446 [1]; 409[6]			
8bc	16/3-2	N	Granite	456	949.7	48.8	2.680
9bc	16/4-1	N	Granite	460	88	6.9	2.646
10bc	16/5-1	N	Granite	463	179.8	11.3	2.662
11abc	16/6-1	N	Porphyric volcanic rock	447 [45]; 430	181.1	9.5	2.591
12a	210/4-1	UK	Biotite gneiss	442 [2]			
13a	BGS81/17	UK	Hornblendite	697 [13]			
14a	211/26-1	UK	Biotite–garnet gneiss, greenschist	430			
15a	9/4-1	UK	Hornblendebiotite schist	393 [7]			

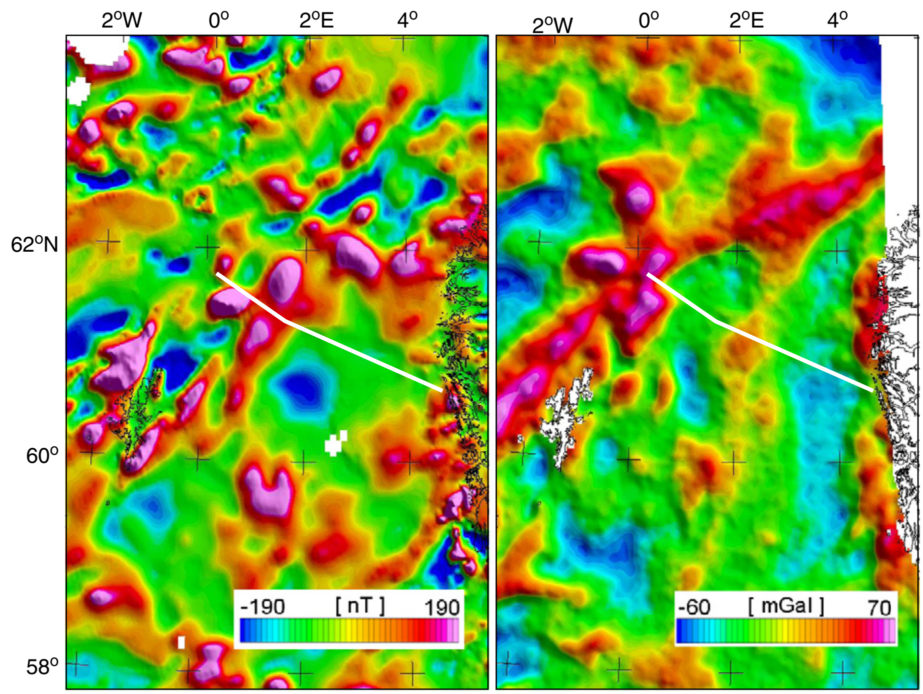

Fig. 2. Maps of magnetic (left) and free air gravity (right) data covering the northern North Sea and adjacent areas with location of modeled deep seismic line NSDP84-1.

data, which was therefore smoothed with a Butterworth low pass filter (cutoff wavelength 20 km, filter degree 8). The vertical gradient of the magnetic data could be used without smoothing. For simplification, the magnetic modeling was restricted to induced magnetization. This is a reasonable approach for this area, as most of the rock types of the interpreted area have intermediate to low magnetic remanence (e.g., Clark, 1997). The error introduced by this simplification concerns size and shape of the few mafic intrusives, which is of minor importance for the overall crustal understanding. Profile oriented, so called 2D gravity and magnetic modeling has been performed. This technique computes the gravity and magnetic anomalies under the assumption, that the structures shown in the depth section strike in a vertical angle off the section in the map plane (Rasmussen and Pedersen, 1979; Talwani et al., 1959). The bodies forming the easternmost and westernmost part of the modeled section, were horizontally continued, in order to avoid boundary effects. The processing and presentation of the maps as well as the 2D gravity and magnetic modeling were performed in GEOSOFT software with the modules Oasis Montaj and GMSYS2D, respectively.

Modeling constraints included mapped seismic layers, i.e., the sedimentary boundaries, the top basement and the Moho from the deep seismic section NSDP84-1 with line drawings which were redrawn from Christiansson et al. (2000) in Fig. 3. Crustal velocities in form of depth–velocity curves from Christiansson et al. (2000) were also included (Fig. 3). Further constraints are the density averages of major sedimentary layers from Statoil's well database (Fig. 4). The “magnetic susceptibility” is in the following text abbreviated to “susceptibility”. The susceptibility of sediments in general (Clark, 1997) and in the North Sea is small (Mørk et al., 2002) compared with common crustal rocks and it is therefore a reasonable simplification

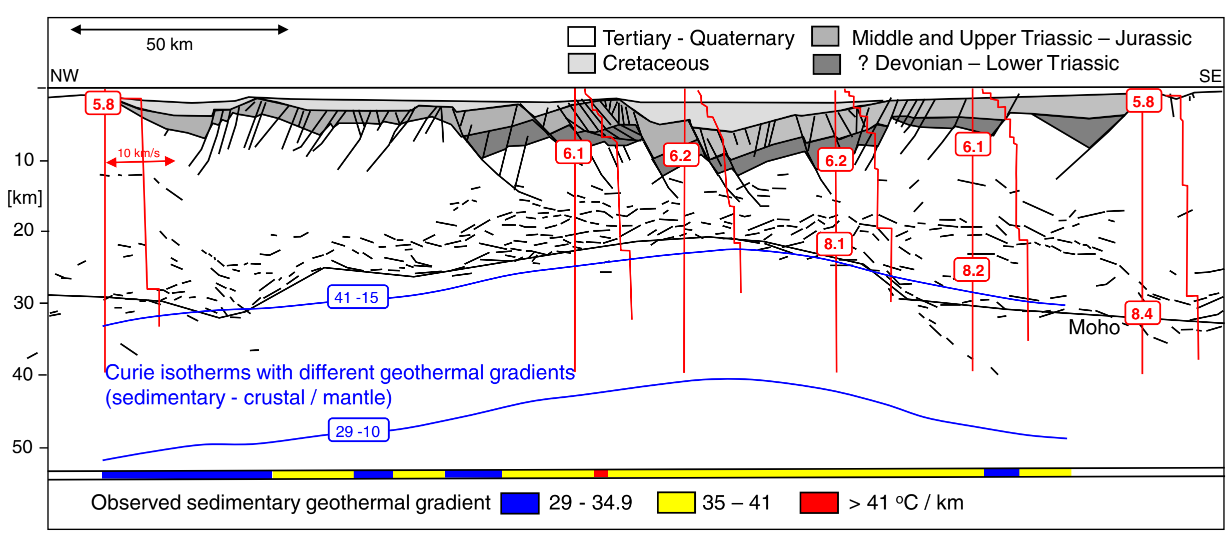

Fig. 3. Line drawing of the deep seismic section NSDP84-1 and its velocities (red) from Christiansson et al. (2000), superimposed is the estimated range of the present day Curie Isotherm for magnetite (580 °C; blue; numbers in box are sedimentary and crustal geothermal gradients in °C/km); observed sedimentary geothermal gradient extracted from Kubala et al. (2003), base of figure.

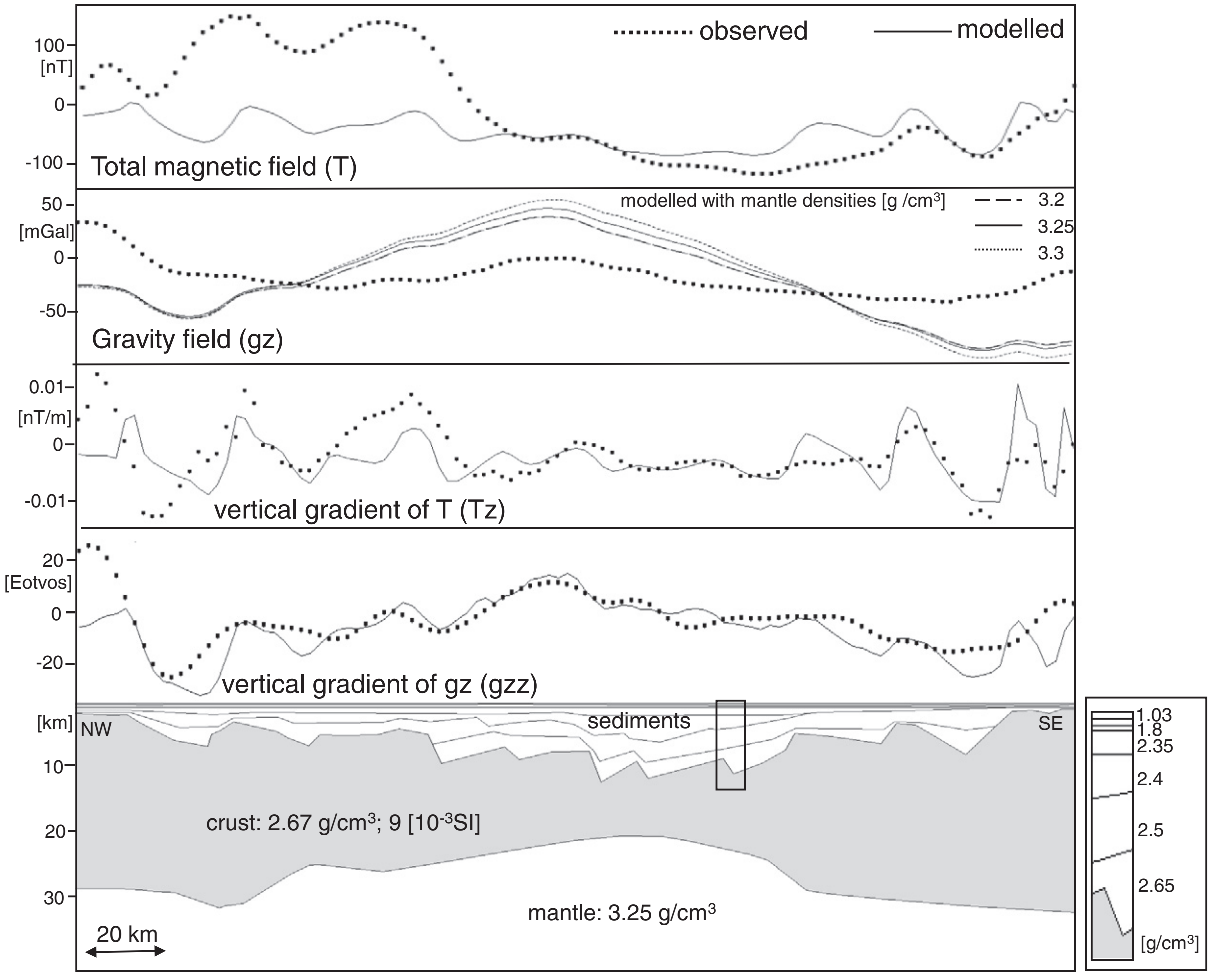

Fig. 4. 2D modeling result for NSDP84-1 assuming a constant crustal density and susceptibility honoring the basement well cores (Fig. 1, Table 1). Sedimentary densities relate to Statoil's well database. Main findings are the mismatch of gravity and magnetic anomalies, whereas its gradients give a reasonable match indicating a more complex crust at greater depths. Modeling results for the gravity anomalies with different mantle densities are also shown and give only minor changes in the regional trend.

to set these susceptibilities to zero. The mantle density was chosen to 3.25 g/cm^3; this choice is discussed in more detail later in the text. The susceptibility of the mantle was set to zero, which is a valid value for peridotites (cf., Clark, 1997). The modeling was thereby restricted to crustal structure between top basement and the Moho.

Prior to the modeling of magnetic data, the lower depth limit for magnetic sources was estimated, which is defined by the Curie temperature. The most abundant magnetic mineral is magnetite with a Curie temperature of 580 °C (cf., Hunt et al., 1995). As there are no direct measurements, a coarse estimation of the depth range of the Curie isotherm was performed using geothermal gradients. The geothermal gradients of sediments along NSDP84-1 were extracted from the map of Kubala et al. (2003; Fig. 3). The sedimentary gradients are in the range between 29 and 41 °C/km. The gradients in crust and mantle are constrained by the thickness of the lithosphere estimated between 80 km and 130 km from seismological data (Artemieva et al., 2006). Additionally, the average onshore geothermal gradient for southern Norway, 10 °C/km (Pascal and Olesen, 2009), is regarded as the lowermost limit. It was therefore assumed, that the average geothermal gradient below the sediments is between 10 and 15 °C/km. The shallowest as well as the largest depths for the Curie isotherm were calculated based on the highest and lowest gradients in sediments and crust, respectively. A smoothed depth to basement was utilized for the calculation. This simple approach indicates a Curie depth near to or below the Moho (Fig. 3). Such depths are also in accordance with the modeling of the thermal evolution by Odinsen et al. (2000).

In the first step of modeling the complexity of the crust is investigated. For this purpose, a constant density and susceptibility were applied, valid for felsic rocks types, which are found in abundance in the North Sea (Fig. 1). The upper crustal density and susceptibility were chosen according to measured values from basement well cores (Table 1). The modeling result (Fig. 4) showed a distinct misfit for the gravity and magnetic anomalies. The mantle densities were varied between 3.2 and 3.3 g/cm^3, corresponding to harzburgitic and lherzolitic mantle rocks, respectively (Hacker et al., 2003). These values slightly changed the regional trend for calculated gravity (Fig. 4), but this effect cannot account for the misfit and was also regarded of minor importance for the overall modeling result. Therefore, for the further modeling, a value of 3.25 g/cm^3 was chosen. However, a good match was observed for the vertical gradients, which represent the short wave length anomalies mainly related to the highly faulted top basement topography. We could therefore conclude, that the applied density and susceptibility are, with minor adjustments, a reasonable choice for the upper crust, whereas more complexity is needed in the deeper part of the crust.

The crust is therefore divided into two layers. Honoring the inherent ambiguity of potential field data, we present three models, which all give a good match to the gravity and magnetic data and its gradients (Figs. 5 and 6). The upper crust was divided into blocks with

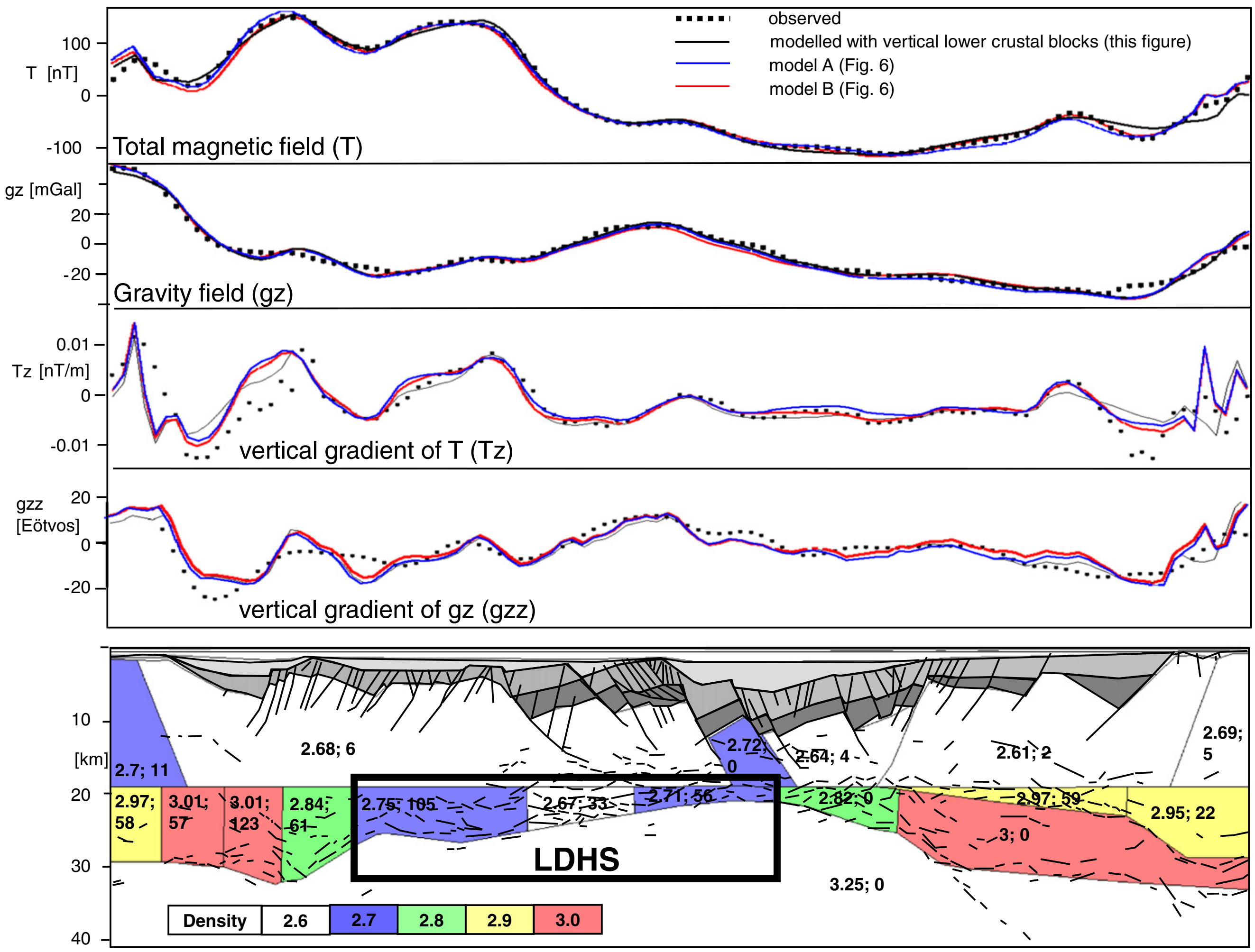

Fig. 5. 2D modeling results for three different models (this figure and Fig. 6) which all give a good fit for the gravity and magnetic anomalies as well as its gradients. The upper crustal parameters are mainly sensitive to the gradients and are kept constant for all models. The lower crust in the simplest possible model (lower image) is divided into vertical blocks. First value within each unit is density (g/cm^3), second value magnetic susceptibility (10^{-3} SI); LDHS = zone of low density, very high susceptibility and opposite polarity of gravity and magnetic field anomalies.

its boundaries defined by major fault zones, where possible. A good fit, especially for the gradients, was achieved with densities and susceptibilities varying between 2.61 and 2.72 g/cm^3 and 0 and 0.011 SI, respectively. These values were kept constant for the three different models.

The simplest possible model is given in Fig. 5. The lower crust was divided into vertical blocks with laterally varying density and susceptibility. The lower crustal body (LCB) in the eastern part of the section, whose top is defined by the jump to mantle type velocities of 8.1–8.4 km/s, is included with a density of 3.0 g/cm^3. The parameters of the easternmost block on top of the LCB were kept within the range of onshore values from the Western Gneiss Region, allowing densities between 2.75 and 2.95 g/cm^3 and susceptibilities between 0.03 and 0.01 SI (Olesen et al., 2010).

An important result was the very high susceptibilities combined with low densities found below the East Shetland Basin, indicated as “LDHS” zone in Fig. 5. The area of low densities extends over the entire East Shetland Basin and the western part of the Viking Graben, whereas the susceptibilities decay to very small values in the deepest part of the Viking Graben. An understanding of this area is the focus of this paper and the model refinement aimed on these structures.

In order to match the anomalies, both the geometry and the assigned parameters of the structural sources (bodies) can be modified, which allows a high degree of freedom. Structurally meaningful bodies should honor the structure indicated by the reflectivity pattern. Reflectivity in the lower crust has been attributed to petrologic heterogeneities according to synthetic seismic modeling by Warner (2004) or to fault planes and fractures including, e.g., a delamination model (Odinsen et al., 2000). The models in Fig. 6 are identical apart from the bodies marked by 1, 2 and 3. In model A, these bodies were kept small, in model B, these bodies were as large as regarded reasonable; which resulted in moderate and low densities for basement rocks, respectively. However, the susceptibility in both models, has to be classified as very high. Low to intermediate densities, combined with high susceptibilities are rock parameters commonly associated with serpentinites. Prior to the petrologic interpretation, a review of serpentinites and meta-peridotites is given.

5. Rock parameters and characteristics of serpentinites and meta-peridotites

Serpentinites are hydrated mantle rocks; the serpentinization reaction transforms peridotites by hydration into serpentinites. The availability of water determines the reaction, which commences in the subsurface at moderately elevated temperatures and pressures (e.g., Winter, 2009). Dehydration of serpentinites (de-serpentinization)

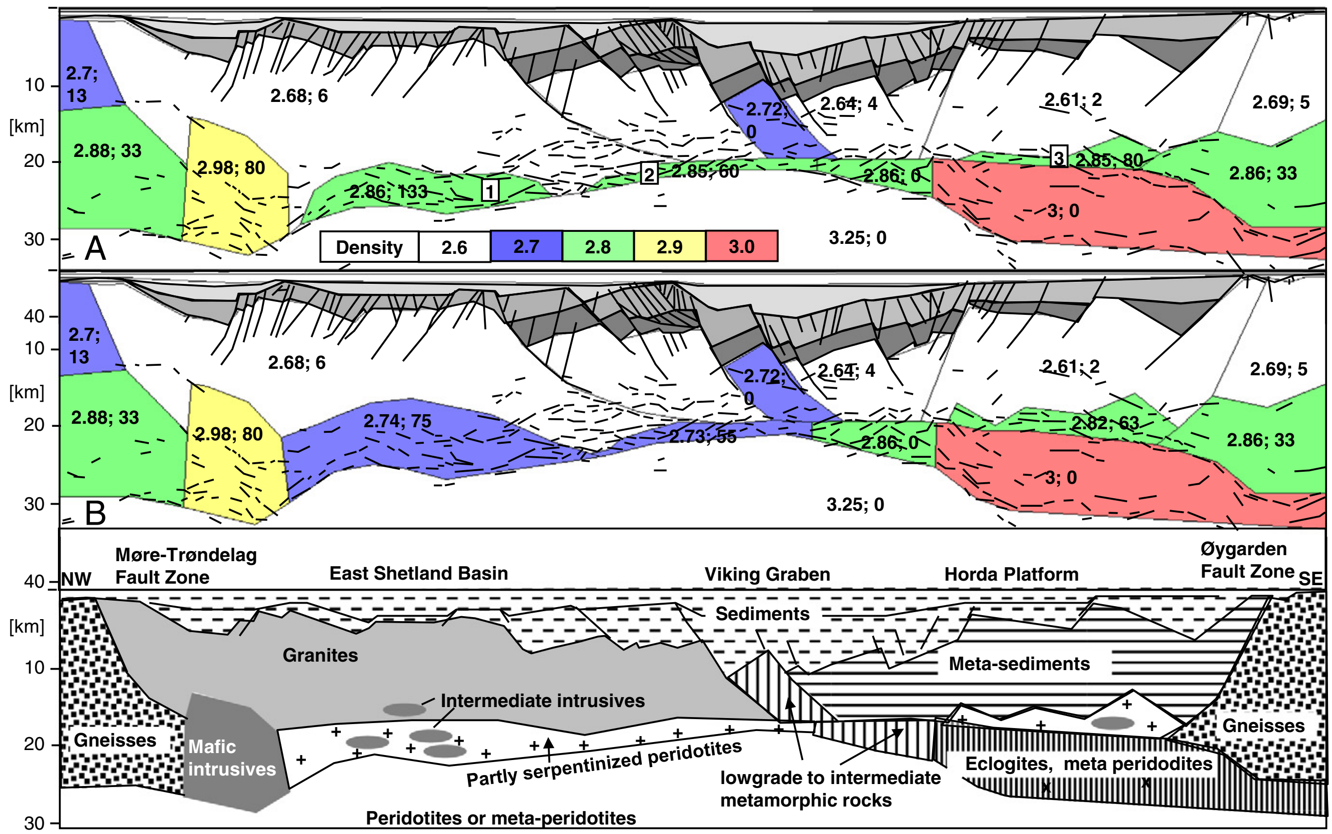

Fig. 6. Modeled crustal sections A and B (upper and middle figure) which fit the gravity and magnetic anomalies and its gradients as shown in Fig. 5. The structure was chosen according to the pattern of the line drawings. First value within each unit is density (g/cm^3), second value magnetic susceptibility (10^{-3} SI). The lowermost section shows the petrologic interpretation.

which transforms the serpentinites back to peridotite (meta-peridotite) is solely driven by the increase of pressure and temperature (Hacker et al., 2003; Seibold and Schilling, 2003; Winter, 2009). As seen in Fig. 7, this process happens at temperatures and pressures below the melting of wet granite. De-serpentinization is a rather instant process and associated with a de-serpentinization front and high pressure fluid release (Chollet et al., 2011; Conolly, 2010; Jamtveit and Austrheim, 2010; Seibold and Schilling, 2003).

Seismic velocities, densities, and magnetic attributes of serpentinites are presented in Fig. 8 versus the fraction of serpentinite in the serpentinized rock. Both seismic velocities and densities show a linear decrease with serpentinized fraction (Escartin et al., 2001; Miller and Christensen, 1997). Susceptibilities show a generally high spread and are characterized by a slow increase for serpentinized fractions lower than 0.6, and a strong increase at higher fractions (Coleman, 1971, Kelso et al., 1996). This has been explained by a change in the serpentinization reaction upon releasing iron (Oufi et al., 2002). The susceptibilities of the serpentinites are due to magnetite formed during the serpentinization reaction by the breakdown of the iron-rich olivines (fayalites). Fayalites are paramagnetic and a typical value is 0.001 SI (Clark, 1997). The percentage of fayalite in the peridotite can vary quite much (e.g., Winter, 2009) and is therefore another factor, which adds to the large uncertainties in the susceptibilities. De-serpentinization sets the densities and velocities back to peridotite values, as shown in Fig. 7. The scarce observations indicate that meta-peridotites have the very low susceptibilities of peridotites (Clark; 1997; Shive et al., 1988). The magnetic remanence of serpentinites is low (Oufi et al., 2002).

Geological characteristics of meta-peridotites are described here in more detail as their occurrence and description in the literature is scarce. Outcrops are found at the Almklovdalen ultramafic body in the WGR which is exposed due open pit (surface) mining of olivine. Osland (1997) has mapped these outcrops and has documented a variety of meta-peridotites, secondary serpentinite, dunite, chlorite,

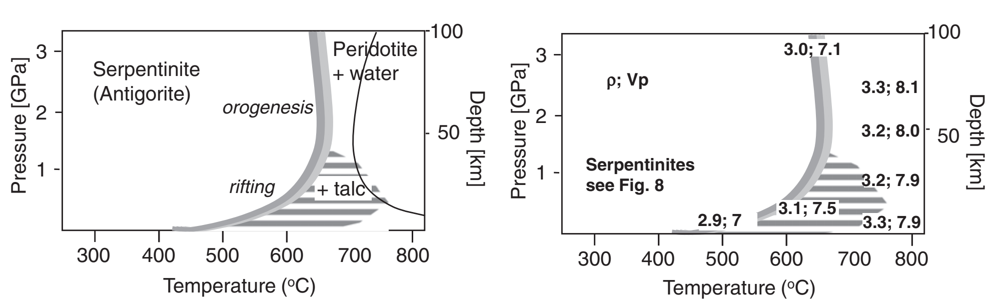

Fig. 7. Pressure–temperature diagram of serpentinites and meta-peridotites (Hacker et al., 2003; Seibold and Schilling, 2003); right: with densities ρ (g/cm^3) and P-wave velocities Vp (km/s) from Hacker et al. (2003). The thin line in the left figure is the melting curve of wet granite.

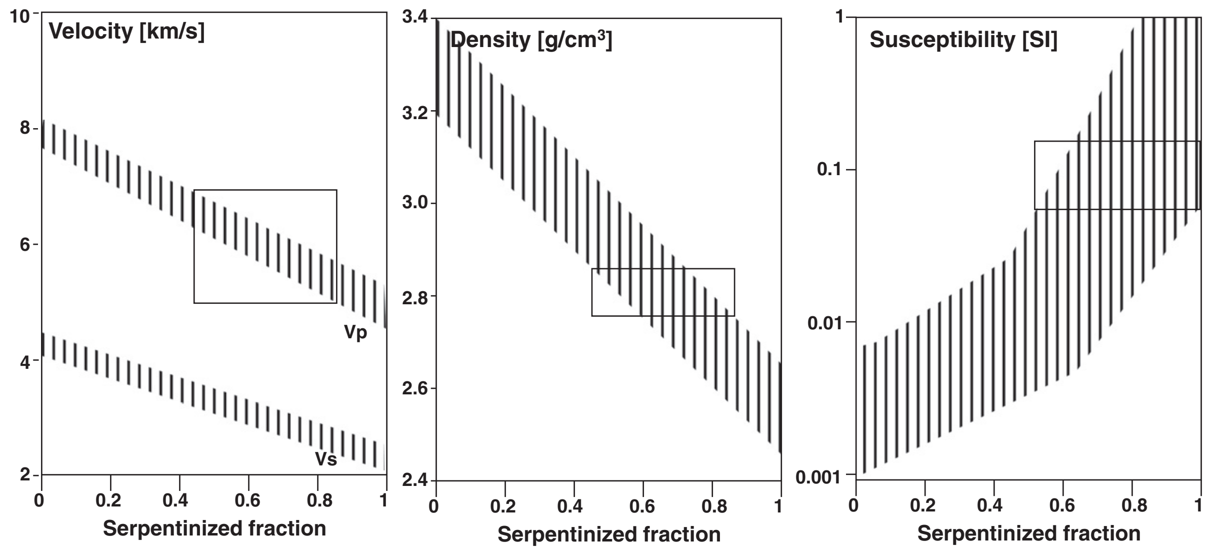

Fig. 8. Compilations of seismic velocities for P- and S-waves (Vp, Vs), densities (Escartin et al., 2001; Hacker et al., 2003; Miller and Christensen, 1997) and magnetic susceptibilities (Clark, 1997; Coleman, 1971; Kelso et al., 1996) for serpentinites; boxes mark the area of the possible model values found for the bodies 1,2 and 3 in Fig. 6.

talc and eclogite. Fluid infiltration pipes from de-serpentinization have also been found (Brueckner, 2009; Kostenko et al., 2002). Meta-peridotites are highly heterogeneous on an outcrop scale due to focused fluid movements and thereby focused metamorphic reactions. Such rock types may contribute to chaotic seismic reflectivity. Grønlie and Rost (1974) have found a density of 3.22 g/cm^3 for the Almkløvdalen ultramafic body as an average for the sampled rocks and valid for their gravity modeling. This is in the same range as typical mantle densities – and can – on the large scale of our model not be distinguished from original mantle rocks.

6. Crustal petrologic interpretation

In the next step, the modeled sections were interpreted in terms of crustal petrology (Fig. 6), which included as well as challenged the possible occurrence of serpentinites and meta-peridotites. Our interpretation of the rocks other than the serpentinites described above relied on published densities and susceptibilities from offshore well data (Table 1), onshore Norway (Olesen et al., 2010) and general rock tables for densities (e.g., Dobrin and Savit, 1988; Hacker et al., 2003) and susceptibilities (Clark, 1997). The interpretation is shown in Fig. 6. We are aware, that very high susceptibilities may be a misinterpretation of high magnetic remanence, but this is regarded to be of minor importance for this rather qualitative petrologic interpretation.

The upper crust west of the Møre-Trøndelag Fault Zone, is characterized by low to intermediate density and susceptibility, which may indicate gneisses or low or intermediate grade metamorphic rocks (greenschist to amphibolite facies). East of this block, a large unit extending from the Møre-Trøndelag Fault Zone into the Viking Graben has low densities and susceptibilities which match with the parameters of granites, which have been found in wells in this area (Fig. 1). The central block in the Viking Graben has an intermediate density and a very low susceptibility. This fits with gneisses or mafic metamorphic rocks (greenschist facies). The eastern part of the Viking Graben has very low densities and very low susceptibilities, which fits with granitoid rocks including granites, quartzites, breccias and metasediments. The next block under the Horda Platform has even lower values. The density of 2.61 g/cm^3 is at the limit of possible crustal rocks, which may indicate, that either the top basement is deeper or the density of the sediments is locally too high. The easternmost part may belong to the offshore prolongation of the WGR as has been documented further north by well results (Fig. 1, Table 1). The modeled intermediate densities and low susceptibilities fit with gneisses expected in such a setting.

The lower crust is complex and laterally varying along the profile. The lower crust of the westernmost area of the East Shetland Basin is characterized by high density and intermediate to high susceptibility which is typical for mafic intrusives or mafic metamorphic rocks (amphibolite–granulite facies) or gneisses. Immediately to the east and in the area of the Møre Trøndelag Fault Zone, a block of very high density and susceptibility was found. The magnetic anomaly in the map plane which belongs to this block, is offset to the depth section, as seen in Fig. 2 or 10. The body is therefore located off the section and will not be visible in the deep seismic line, which may explain its somewhat uncorrelated occurrence with the structure on the section. The lower crust below the East Shetland Graben which extends to the deepest part of the Viking Graben was modeled as a unit of low to intermediate density and very high susceptibilities, which fits in both models A and B (Fig. 6) with serpentinites with a fraction between 0.4 and 0.8 as shown in Fig. 8. The intermediate densities and high susceptibilities in model A can also be explained by intermediate intrusives or a combination of both intrusives and serpentinites.

East of this area, under the eastern Viking Graben a lower crustal block with intermediate density and very small susceptibility is found. This fits with mafic metamorphic rocks, (greenschist to amphibolite facies), but gneisses are also possible. East of this area is the LCB with its very high velocities and consequently high densities. Its susceptibility is very low, which supports the interpretation of Christiansson et al. (2000), describing this as ultra high pressure mafic metamorphics, including eclogites. On top of the LCB, in the middle of the crust, another body is located with intermediate densities and very high susceptibilities. It is similar to the lower crust below the East Shetland Basin and may therefore be serpentinite, intermediate intrusives or a combination of both. Finally, the easternmost crustal block has densities and susceptibilities, which are very similar to the westernmost lower crustal block and are characterized in the same manner as mafic intrusives or amphibolite–granulite facies metamorphic mafic rocks or gneisses.

7. Tectonic interpretation

In this final part of the interpretation, the tectonic history was included in order to further evaluate the petrologic interpretation with special focus on serpentinites. The suggested serpentinite zone was outlined by the combination of high magnetic anomalies with low gravity anomalies. This zone can be tracked in the map plane striking in NNE–SSW direction over a length of at least 200 km as shown by the white dotted line enclosing these anomalies in Fig. 9. It forms a major part of the East Shetland Basin.

Serpentinites have low viscosities (Escartin et al., 2001). They have been shown to develop into serpentinite myllonites in fault zones, (e.g., Alexander and Harper, 1992; Moore and Lockner, 2008) and may therefore support the generation of detachment faults. A supporting argument for the occurrence of serpentinites may therefore be found in the large detachment fault forming the western graben shoulder of the Viking Graben (Fig. 6), with the lower part of the fault plane along the suggested serpentinite. Furthermore, it can be speculated, whether the series of southeast ward dipping faults may has been supported during its generation by serpentinites (Fig. 9). Another argument for serpentinization or dehydration of serpentinites is seen in Re–Os isotopes related to Jurassic source rocks, which indicate contact with mantle fluids during their deposition (Finlay et al., 2010). The indicated mantle fluids may be related to the hydrothermal systems of serpentinization or dehydration of serpentinites during the rifting. The locations of these findings are shown in Fig. 9, and two of the occurrences are very near to the large detachment fault discussed above, a third occurrence is found further west, also within the zone outlined as possible serpentinites.

Serpentinites in the North Sea basement can be inherited or be generated in situ. The mechanism for in situ generation of serpentinites requires contact of water with the mantle, typically happening by deep crustal faulting in hyper-extended settings (Abe, 2001; Lavier and Manatschal, 2006; Perez-Gussinye and Reston, 2001). Hyper-extension has not been supported in the North Sea according to sedimentary reconstruction (Giltner 1987; Gabrielsen et al., 1990; Færseth et al., 1995; Roberts et al., 1995; Kyrkjebø et al., 2001). However, the rather thin layer of suggested serpentinite below the heavily faulted Viking Graben may have been generated by water penetrating the deep crust and uppermost mantle from above. This mechanism is less probable for the serpentinites suggested in the lower crust under the East Shetland Basin, because there is less deep faulting as well as a larger amount of serpentinites. According to Fig. 9 and the model in Fig. 6, this gives, coarsely estimated, a volume of 5 × 50 × 200 km. Therefore, inherited serpentinites may be considered. Their origin requires a closer look on the Iapetus Ocean and the collision of Baltica and Laurentia.

Possible origins of inherited serpentinites include: (1) hydrothermal fields near slow spreading mid oceanic ridges (Kelley et al., 2005), (2) forearc of continental subduction (Blakely et al., 2005; Bostock et al., 2002; Hyndman and Peacock, 2003; Puchkov, 2009), and (3) forearc of island arc subduction (Arai et al., 2004; Kido et al., 2002, 2004). Hydrothermal fields (1) cannot produce enough serpentinites to fit our interpreted volumes. Forearc serpentinization of continental subduction (2) will have happened, while Baltica is pushed underneath Laurentia in the Caledonian collision. The LCB has been interpreted by Christiansson et al. (2000) as an exhumed subduction slab of the Caledonian orogeny with a major content of eclogites. Our interpretation opens for additional amounts of meta-peridotites. The LCB could be of similar petrology as the Almklovdalen ultramafic body. If the LCB is a part of the mountain root, as suggested by Christiansson et al. (2000), its burial will have brought this unit to p-T conditions of the meta-peridotite zone as shown in Fig. 7. Serpentinites will have been generated by the dehydration of this slab in the overlying mantle rocks. According to this model, serpentinites will be expected directly over the LCB, which matches the location of the observed body nr.3 in Fig. 6. Above such a slab or generally adjacent to the Caledonian orogeny, a trench is expected which will be filled with erosional material from the mountain chain. This could be the origin of the upper crustal unit below the Horda Platform, which was interpreted as meta-sediments (Fig. 6).

We argue in the following, that a plausible explanation for the bodies 1 and 2 in Fig. 6 below the western Viking Graben and the East Shetland Basin is forearc serpentinization caused by island arc subduction. The mantle wedges of oceanic and continental subduction zones are a major factory for serpentinites (Kido et al., 2002, 2004; Arai et al., 2004; Hacker et al., 2003; Hyndman and Peacock, 2003; Bostock et al., 2002). Hyndman and Peacock (2003) have reviewed the origin and growing evidence for subduction forearc serpentinites. A short summary of their findings is given here as well as illustrated in Fig. 10. Large volumes of aqueous fluids are released upwards from the subducting slab of oceanic crust and sediments. The fluid release is

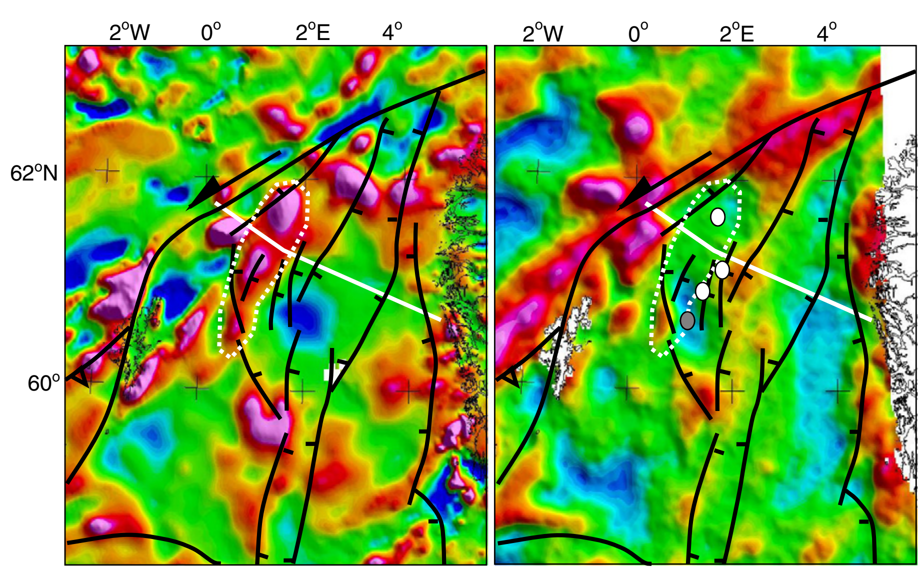

Fig. 9. Maps of magnetic (left) and free air gravity (right) data, superimposed are the location of modeled deep seismic line NSDP84-1 (white) and major faults (Coward, 1990; Gabrielsen et al., 1999; Zanella and Coward, 2003; Fig. 1). The white stippled line encloses a string of anomalies of high magnetic and low gravity anomalies. This area is interpreted along the profile as serpentinites, and outlines as such a zone of possible serpentinites in the map plane. Its origin is suggested to be an inherited island arc chain. Superimposed on the gravity data are locations, where oils, sourced from Jurassic rocks, have been analyzed with respect to Re–Os isotopes. White circles indicate contact with mantle fluids (Finlay et al., 2010).

caused by both compaction and by low temperature–high pressure metamorphic reactions of both sediments and oceanic crust. Subduction of oceanic lithosphere cools the overlying forearc such that serpentine minerals are stable in the forearc mantle. The width of the serpentinite zone varies from 50 to 150 km, and the maximum vertical extension of the wedge between 30 and 50 km. The fluid infiltration is described as a heterogeneous process. It has been shown by geophysical modeling that the forearc mantle is serpentinized in average by a fraction of 20%; locally, 50% may be reached. Evidence for ongoing serpentinization in subduction forearc mantle has been found in the Mariana Island Arc by the ODP drilling project with mud volcanoes at the seabed build up of low-temperature, fine-grained unconsolidated serpentine flows (Fig. 10; Fryer, 1992; Mottle, 2009).

During late Ordovican, not only the island arcs of the Iapetus Ocean, but also the associated serpentinite wedges will have been assembled at the western boundary of Baltica. The process of assemblage is sketched in Fig. 11a following drawings of Keary and Vine (1996) and Fossen et al. (2008), to which we added serpentinized mantle wedges. The next phase, shortly before the closure of the Iapetus Ocean is sketched in Fig. 11b. Instead of hypothetical Caledonian sketches for this phase (e.g., Andersen et al., 1991; Fossen, 2000; Hacker, 2007; Rey et al., 1997) we show a present day analog as it exposes substantial amounts of assembled serpentinites at the surface: the Moroccan Alpine Rif Belt (Chalouan and Michard, 2004).

A further argument for an island arc is found on the gravity and magnetic maps. The marked zone of suggested serpentinites shows a regular string of positive magnetic maxima in the map plane coinciding with an area of low gravity values without internal structuring (Fig. 9). The distance between adjacent magnetic anomalies is approximately 65 km and thereby well within the range of the periodicity of resent island arc volcanoes. Similar periodicity in gravity and magnetic anomalies has been observed and linked to forearc serpentinites at the Japanese Island Arc (Kido et al., 2002, 2004). The maxima of the magnetic field within this zone will in such a model be related to intermediate intrusives, typically found in island arcs (Winter, 2009).

It has to be noted, that the serpentinized fraction of the suggested serpentinite unit is larger than expected for forearc mantle wedges as described above. A possible explanation may be secondary serpentinization by water released by prograde metamorphism during the Permian and Jurassic rifting. The suggested serpentinite bodies (1 and 2 in Fig. 6) are also less in volume as expected for a whole serpentinized mantle wedge as sketched in Fig. 10. The deep parts of this mantle wedge will have experienced high enough pressure and temperature to be de-hydrated (Fig. 7) and will as such be a source of water. The metamorphic reaction from serpentinite to meta-peridotite takes place at different depths in an orogen compared with a rift setting as shown in Fig. 7. Orogenic conditions normally include a low geothermal gradient (e.g., Warren et al., 2008), and an average of 15°/km has been suggested by Rey et al. (1997) for the Caledonian orogeny. Thus, serpentinites will remain stable at depths shallower than 50 km as shown in Fig. 7 but are transformed into meta-peridotites at greater depths. Rift settings typically have higher geothermal gradients and will therefore cause a transition from serpentinites to meta-peridotites at shallower depths. A reasonable estimate for a rift setting is an average geothermal gradient between 20 and 50°/km. Such crustal gradients have been found in the non-volcanic rift of the German Upper Rhinegraben (Lampe and Person, 2002). Similar values are also found for the active Red Sea rift (Aboud et al., 2011). In such a setting, the transition to meta-peridotites, should occur at about Moho depths. We can therefore expect, that appreciable amounts of serpentinites have survived the Caledonian orogeny, but have later been transformed to meta-peridotites in the subsequent rift phases. The serpentinite body outlined by our modeling is therefore assumed to be a minor part of the originally serpentinized mantle wedge, left over after de-serpentinization of the rifting and the orogeny.

It is noted, that the upper crustal unit, which was interpreted as possible granitic body covers approximately the same area as the suggested serpentinite body, which may therefore be interpreted as the shallow part of the suggested island arc. Such rocks with the calc alkaline character of island arc rocks have been found south of our study area at the Utsira High (Slagstad et al., 2011).

An anti model to serpentinites in the lower crust was already mentioned and such a model would explain all of the modeled rock parameters of bodies 1, 2 and 3 in Fig. 6 by intermediate intrusives. This model is fully compatible with the modeled densities and susceptibilities. However, its tectonic history has to be discussed, honoring their location under the East Shetland Basin as well as the lack of these rocks under the deepest part of the rift, the central Viking Graben. In the first step, we compare the location of the intrusives with the expected location according to standard rift models. The symmetric rift development according to the McKenzie model (McKenzie, 1978; McKenzie and Bickle, 1988) would expect intrusives under the deepest part of the rift. This is not observed. Furthermore, the suggested intrusives do neither fit with the Wernicke model (Wernicke, 1985), where the intrusives are expected

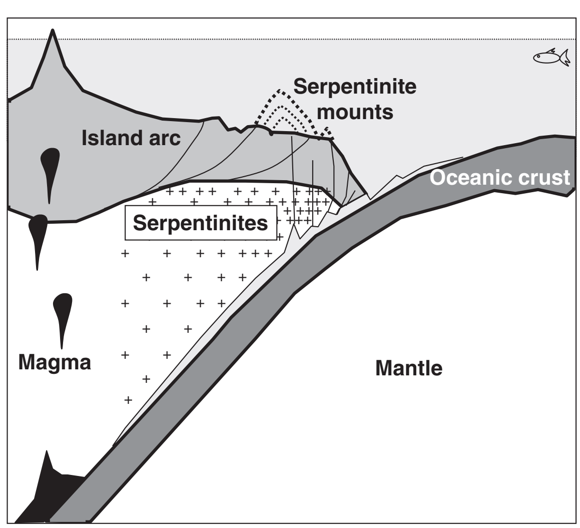

Fig. 10. Sketch of an island arc with its serpentinized mantle wedge formed by the release of fluids from the subducted slab; based on sketches from. Fryer (1992), Hyndman and Peacock (2003) and Winter (2009). Area with crosses indicates mantle rocks with serpentinites.

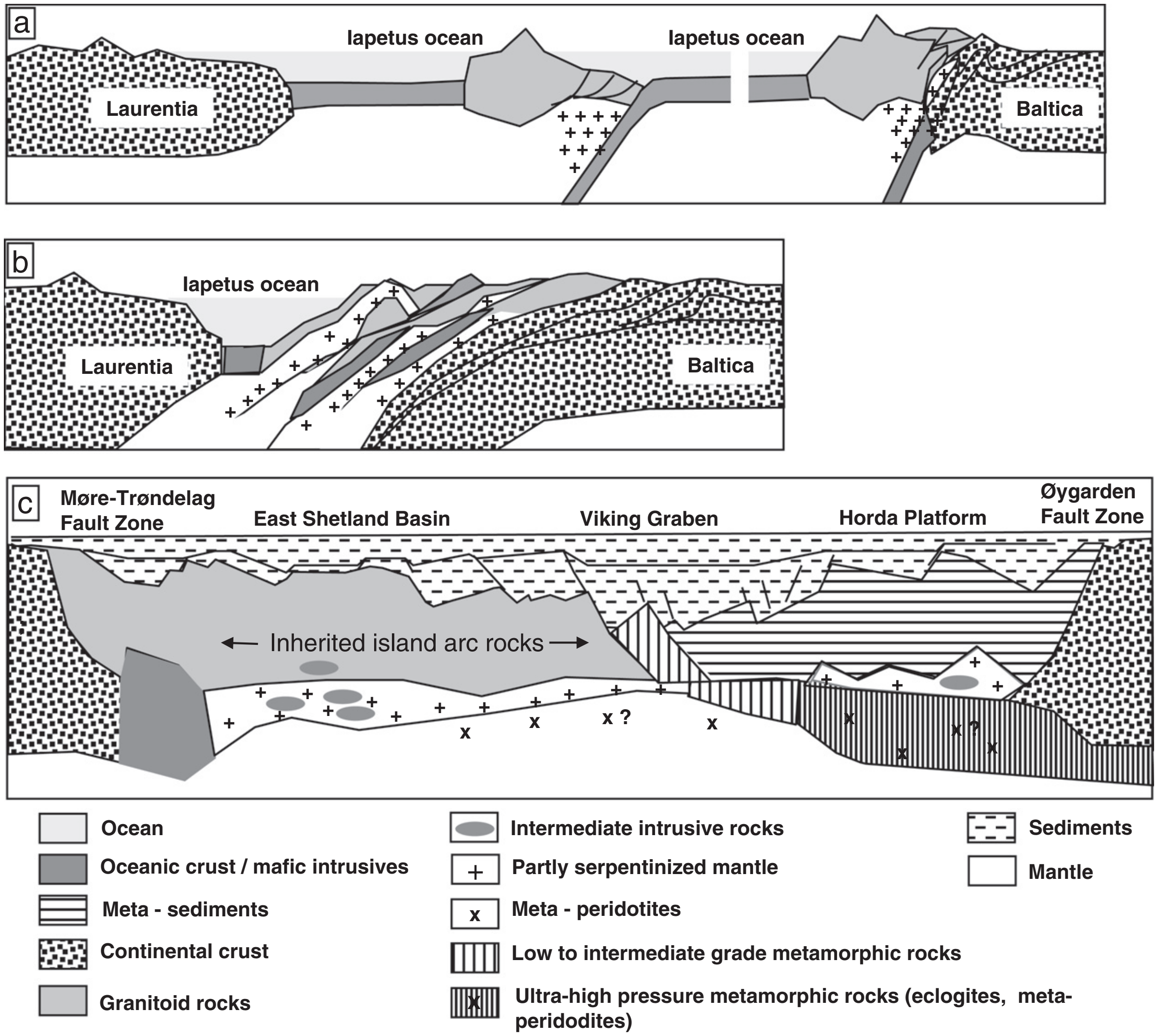

Fig. 11. Formation of inherited structures in the North Sea Crust with focus on serpentinites and meta-serpentinites; (a) late Ordovician (Fossen et al., 2008; Keary and Vine, 1996; Winter, 2009), (b) Middle Silurian (Wenlock) is shown in its eastern part in form of an analog, the alpine Rif Belt put into our setting (Chalouan and Michard, 2004), (c) present day by our model from Fig. 6.

at the lower end of the master detachment fault, which would here be in the area adjacent to the LCB. Finally, the recent model of magma compensated crustal thinning (Thybo and Nielsen, 2009) would also expect most of the intrusives under the central area of the rift, which is not observed here. It was therefore concluded, that the suggested intrusives are possibly of older age, i.e., synorogenic intrusions during the orogenesis of the Caledonides or inherited intrusions of even older age. Bodies 1 and 2 may in the setting of a string of anomalies as discussed above (Fig. 9) be due to island arc magmatism. Body 3 on top of the LCB, which is interpreted as exhumed slab by Christiansson et al. (2000), may be synorogenic intrusives, caused by the slab dehydration, but an older age and an inherited character is also possible.

Fig. 11 presents our results in a plate tectonic perspective. The first sketch shows the development of the area starting with the island arcs and its subduction wedges in the Iapetus Ocean. The next sketch relates to its assemblage with Baltica prior to the collision with Laurentia. Here, we use the Alpine Rif Belt (Chalouan and Michard, 2004) as analog as described above. The lowermost sketch corresponds to our model, as a result after reworking and metamorphism during the Caledonian orogeny and subsequent rifting. This model would be valid for both serpentinites and intermediate intrusives in the lower crust, and a combination of both models is possible and regarded as probable.

8. Discussion

Our hypotheses of serpentinites versus intermediate intrusives in the deep crust could be further tested by including more geophysical data as, e. g., crustal seismic velocities.

Geological consequences of the serpentinites with respect to structural geology may include weakening of the crust caused by the high viscosity of the serpentinites. One effect may be the physical support for the generation of faults. Another effect on a large scale may be on the response of the rift area to compressional deformation. Lundin and Doré (2011) discussed this effect for serpentinized hyper-extended margins. Furthermore, serpentinite bodies at the transition between crust and mantle may – in an appropriate margin setting – support the initiation of hyperextension by providing a gliding plane due to high viscosity of the serpentinite body.

In terms of plate tectonics, our interpretation may be used to constrain the location of the Iapetus suture. Whereas the location onshore Great Britain as well as in adjacent offshore areas is well constrained (Soper et al., 1992), its prolongation into the northern North Sea is still under discussion. Several suggestions exist, including a location beneath the West Shetland Basin from deep seismic indications (Fichler and Hospers, 1990a,b), as well as a location along the Øygarden fault zone near to the Norwegian coast (Pharaoh, 1999). Our interpretation suggests the location of the main suture to the west of the suggested island arc and east of the Møre-Trøndelag Fault Zone as seen in Fig. 11b.

It is finally noted, that the suggested basement model for the northern North Sea, with inherited and metamorphosed island arc rocks may be of relevance for other basins which developed in areas of ancient ocean closure with similar tectonic settings. This includes many onshore and offshore basins as well as passive margins.

9. Conclusions

1. A new crustal model for the northern North Sea was developed by gravity and magnetic modeling along the deep seismic line NSDP84-1. The usage of gradients allowed a distinction between upper and lower crustal densities and magnetic susceptibilities.
2. The upper crust is characterized by low densities and very low magnetic susceptibilities in the graben areas, which was interpreted by mainly felsic rocks, including granites and metasediments. A block with somewhat higher density, but very low susceptibility was found under the central part of the Viking Graben and was interpreted to lowgrade mafic metamorphic rocks. Toward both the westernmost and easternmost ends of the profile, density and susceptibility show a minor increase and this area was interpreted as gneisses mafic metamorphic rocks (low—to intermediate grade) of continental origin.
3. The lower crust at both the westernmost and easternmost ends of the profile shows high densities and susceptibilities and was interpreted as highgrade mafic metamorphic rocks or gneisses of deep continental origin. A block of very high density and very high susceptibility was found in the area of the Møre-Trøndelag Fault Zone, interpreted as mafic intrusives. The lower crust below the East Shetland Graben as well as the Viking Graben is generally of intermediate density. The area from the western boundary of the East Shetland Basin to the western part of the Viking Graben is characterized by very high susceptibilities, which in combination with the low to intermediate densities can be interpreted as serpentinites or intermediate intrusives. The central and eastern Viking Graben is underlain by rocks of intermediate density and very low susceptibility, interpreted as mafic metamorphic rocks (intermediate grade) or gneisses. The deep crust below the Horda Platform is characterized by two layers. The deepest part is the LCB postulated from the seismic interpretation (Christiansson et al., 2000) with very high densities and very small susceptibilities. The shallower part is characterized as rocks with intermediate to low densities and very high susceptibilities, again indicative for serpentinites or intermediate intrusives.
4. The area indicative for serpentinites or intermediate intrusives can be tracked on gravity and magnetic maps and covers a major part of the East Shetland Basin. Honoring the string of three near equidistant magnetic maxima, which follows the trend of the NNE–SSW striking East Shetland Basin, it is suggested that this area is part of an island arc of the Iapetus Ocean which has been assembled during the collision between Laurentia and Baltica in late Silurian times.
5. The origin of the possible serpentinites under the East Shetland Platform and the western Viking Graben is suggested inherited and related to slab dehydration of an island arc in the Iapetus Ocean. The alternative interpretation concerning intermediate intrusives can be related to the same process, a combination of both is therefore seen as highly probable.
6. The origin of serpentinites or alternatively intermediate intrusives on top of the interpreted continental subduction slab (Christiansson et al., 2000) is suggested related to dehydration of this slab during the collision between Baltica and Laurentia.
7. No indications for magmatism related to the Permian – early Triassic and Jurassic – early Cretaceous rift phases were found along the interpreted profile.

Acknowledgments

We acknowledge the discussions and support by our Statoil colleagues, especially Bjørn Berger, Jan Henrik Borch, Christian Gram, Martin Hovland, Rune Kyrkjebø, Erik Lundin, Trygve Meyer, Tage Røsten, Christopher Stadtler, Bjørn Magne Sæther, Cato Wille and Eli Aamot. Judy Hannah, Hans Konrad Johnsen, Stan Keith, Søren Naumann, Holy Stein and Monte Swan are thanked for inspiration and discussion. We further thank two anonymous reviewers for an excellent review, which certainly improved the manuscript. Finally, Statoil is acknowledged for permission to publish.

References

Abe, N., 2001. Petrochemistry of serpentinized peridotite from the Iberia Abyssal Plain (ODP Leg 173). In: Wilson, R.C.L., et al. (Ed.), Non-volcanic Rifting of Continental Margins: A Comparison of Evidence from Land and Sea: Geological Society special publication, 187, pp. 143–159.
Aboud, E., Salem, A., Mekkawi, M., 2011. Curie depth map for Sinai Penninsula, Egypt deduced from the analysis of magnetic data. Tectonophysics 506, 46–54.
Alexander, R.J., Harper, G.D., 1992. The Josephine ophiolite: an ancient analogue for slow- to intermediate-spreading oceanic ridges. In: Parson, L.M., Murton, B.J., Browning, P. (Eds.), Ophiolites and Their Modern Oceanic Analogues: Geological Society Special Publication, 60, pp. 3–38.
Andersen, T.B., Jamtveit, B., Dewey, J.F., Swensson, E., 1991. Subduction and eduction of continental crust: major mechanisms during continent–continent collision and orogenic extensional collapse, a model based on the south Norwegian Caledonides. Terra Nova 3, 303–310.
Arai, S., Takada, S., MichiBayashi, K., Kida, M., 2004. Petrology of peridotite xenoliths from Iraya Volcano, Philippines, and its implication for dynamic mantle wedge processes. Journal of Petrology 45 (2), 369–389.
Artemieva, I.M., Thybo, H., Kaban, M.K., 2006. Deep Europe today: geophysical synthesis of the upper mantle structure and lithospheric processes over 3.5 Ga. In: Gee, D.G., Stephenson, R.A. (Eds.), European Lithosphere Dynamics: Geological Society, London, Memoirs, 32, pp. 11–41.
Atherton, M.P., Ghani, A.A., 2002. Slab breakoff: a model for Caledonian, Late Granite syn-collisional magmatism in the orthotectonic (metamorphic) zone of Scotland and Donegal, Ireland. Lithos 62, 65–85.
Bassett, M.G., 2003. Sub-Devonian geology. In: Evans, D., Graham, C., Armour, A., Bathurst, P. (Eds.), The Millennium Atlas: Petroleum Geology of the Central and Northern North Sea: The Geological Society of London, London, 5, pp. 1–6.
Beach, A., 1986. A deep seismic reflection profile across the northern North Sea. Nature 323 (4), 53–55.
Blakely, R.J., Brocher, T.M., Wells, R.E., 2005. Subduction-zone magnetic anomalies and implications for hydrated forearc mantle. Geology 33 (6), 445–448.
Bostock, M.G., Hyndman, R.D., Rondenay, S., Peacock, S.M., 2002. An inverted continental Moho and serpentinization of the forearc mantle. Nature 417, 536–538.
Brueckner, H.K., 2009. Subduction of continental crust, the origin of post-orogenic granitoids (and anorthosites?) and the evolution of Fennoscandia. Journal of the Geological Society 166, 753–762.
Chalouan, A., Michard, A., 2004. The Alpine Rif belt (Morocco): a case of mountain building in a subduction–subduction-transform fault triple junction. Pure and Applied Geophysics 161, 489–519.
Chollet, M., Daniel, I., Koga, K.T., Morard, G., Moortèle, v.d.B., 2011. Kinetics and mechanism of antigorite dehydration: implications for subduction zone seismicity. Journal of Geophysical Research 16 (B04203), 1–9.
Christiansson, P., Faleide, J.I., Berge, A.M., 2000. Crustal structure in the northern North Sea; an integrated geophysical study. Geological Society, London, Special Publications 167, 15–40.
Clark, D.A., 1997. Magnetic petrophysics and magnetic petrology: aids to geological interpretation of magnetic surveys. AGSO Journal of Australian Geology and Geophysics 17 (2), 83–103.
Cocks, L.R., Torsvik, T.H., 2003. European geography in a global context from the Vendian to the end of the Paleozoic. In: Gee, D.G., Stephenson, R.A. (Eds.), European Lithosphere Dynamics: Geological Society, London, Memoirs, 32, pp. 83–95.
Coleman, R.G., 1971. Petrologic and geophysical nature of serpentinites. GSA Bulletin 82 (4), 897–918.
Conolly, J.A.D., 2010. The mechanics of metamorphic fluid expulsion. Elements 6, 165–172.
Coward, M.P., 1990. The Precambrian, Caledonian and Variscan framework to NW Europe. In: Hardman, R.F.P., Brooks, J. (Eds.), Tectonic Events Responsible for

Britain's Oil and Gas Reserves: Special Publications of the Geological Society of London, 55, pp. 1–34.
Dewey, J.F., Ryan, P.D., Andersen, T.B., 1993. Orogenic uplift and collapse, crustal thickness, fabrics and metamorphic changes: the role of eclogites. Geological Society of London Special Publication 76, 325–343.
Dobrin, M.B., Savit, C.H., 1988. Introduction to Geophysical Prospecting. McGrawhill, Singapore. 867 pp.
Donato, J.A., Tully, M.C., 1982. A proposed granite batholite along the western flank of the North Sea Viking Graben. Geophysical Journal of the Royal Astronomical Society 69, 187–195.
Ebbing, J., Olesen, O., 2010. New compilation of top basement and basement thickness for the Norwegian continental shelf reveals the segmentation of the passive margin system. In: Vining, B.A., Pickering, S.C. (Eds.), Petroleum Geology: From Mature Basins to New Frontiers—Proceedings of the 7th Petroleum Geology Conference, pp. 885–897.
Escartin, J., Hirth, G., Evans, B., 2001. Strength of slightly serpentinized peridotites: implications for the tectonics of oceanic lithosphere. Geology 29 (11), 1023–1026.
Evans, D., Graham, C., Armour, A., Bathurst, P., 2003. The Millenium Atlas: Petroleum Geology of the Central and Northern North Sea. The Geological Society of London. 390 pp.
Eynon, G., 1981. Basin development and sedimentation in the Middle Jurassic of the northern North Sea. In: Illing, L.V., Hobson, G.D. (Eds.), The Petroleum Geology of the Continental Shelf of North West Europe, Heyden, London, pp. 196–204.
Færseth, R.B., 1996. Interaction of Permo-Triassic and Jurassic extensional fault-blocks during the development of the northern North Sea. Journal of the Geological Society of London 153, 931–944.
Færseth, R.B., Gabrielsen, R.H., Hurich, C.A., 1995. Influence of basement in structuring of the North Sea Basin offshore southwest Norway. Norsk Geologisk Tidsskrift 75, 105–119.
Fairhead, J.D., Green, C.M., Odegaard, M.E., 2001. Satellite gravity having an impact on marine exploration. The Leading Edge 20 (8), 873–876.
Fichler, C., Hospers, J., 1990a. Gravity modeling in the Viking Graben area, North Sea. In: Blundell, D.J., Gibbs, A. (Eds.), Tectonic Evolution of the North Sea Rifts. Oxford University Press, London, pp. 67–77.
Fichler, C., Hospers, J., 1990b. Deep crustal structure of the northern North Sea Viking Graben: results from deep reflection seismic and gravity data. Tectonophysics 178, 241–254.
Finlay, A.J., Selby, D., Osborne, M.J., Finucane, D., 2010. Fault charged mantle-fluid contamination of United Kingdom north sea oils: insights from Re–Os isotopes. Geology 38 (11), 979–982.
Fossen, H., 2000. Extensional tectonics in the Caledonides: synorogenic or postorogenic? Tectonics 19 (2), 213–224.
Fossen, H., Pedersen, R.-B., Bergh, S., Andresen, A., 2008. Creation of a mountain chain. In: Ramberg, I.B., Bryhni, I., Nøttvedt, A., Rangnes, K. (Eds.), The Making of a Land; Geology of Norway. The Norwegian Geological association, Trondheim, pp. 178–232.
Frost, U.E., 1987. The evolution of the Viking Graben tilted fault block structures: a compressional origin. In: Brooks, J., Glennie, K. (Eds.), Petroleum Geology of North West Europe. Graham and Trotman, London, pp. 1009–1024.
Fryer, P., 1992. Mud volcanoes of the Marianas. Scientific American 46–52 Feb. 1992,.
Gabrielsen, R.H., Færseth, R.B., Steel, R.J., Idil, S., Kløvjan, O.S., 1990. Architectural styles of basin fill in the northern Viking Graben. In: Blundell, D.J., Gibbs, A.D. (Eds.), Tectonic Evolution of the North Sea Rifts. Clarendon, Oxford, pp. 158–179.
Gabrielsen, R.H., Odinsen, T., Gunnaleite, I., 1999. Structuring of the Northern Viking Graben and the Møre Basin; the influence of basement grain, and the particular role of the Møre-Trøndelag Fault Complex. Marine and Petroleum Geology 16, 443–465.
Gabrielsen, R.H., Faleide, J.I., Pascal, C., Braathen, A., Nystuen, J.P., Etzelmuller, B., O'Donnel, S., 2010. Latest Caledonian to Present tectonomorphological development of southern Norway. Marine and Petroleum Geology 27, 709–723.
Gibbs, A.D., 1987. Deep seismic profiles in the northern North Sea. In: Brooks, J., Glennie, K. (Eds.), Petroleum Geology of North-West Europe. Graham and Trottman, London, pp. 1025–1028.
Giltner, J.P., 1987. Application of extensional models to the northern Viking Graben. Norsk Geologisk Tidsskrift 67, 339–352.
Glennie, K.W., 1990. Outline of North Sea history and structural framework, In: Glennie, K.W. (Ed.), Introduction to the Petroleum Geology of the North Sea, 3. edition. Blackwell Scientific Publications, Oxford, pp. 34–77.
Grønlie, G., Rost, F., 1974. Gravity investigation and geological interpretation of the ultramafite complex of Åheim, Sunnmøre, western Norway. Publication No. 99 in the Norwegian Geotraverse project, pp. 367–373.
Hacker, B., 2007. Ascent of the ultrahigh-pressure Western Gneiss Region, Norway. Geological Society of America, Special Paper, 419. 14 pp.
Hacker, B.R., Abers, G.A., Peacock, S.M., 2003. Subduction factory: 1. Theoretical mineralogy, densities, seismic wavespeeds and H2O contents. Journal of Geophysical Research 108 (B1), 2029 10-1—10–26..
Holliger, K., Klemperer, S., 1989. A comparison of the Moho interpreted from gravity data and from deep seismic reflection data in the Northern North Sea. Geophysical Journal 97, 247–258.
Holliger, K., Klemperer, S., 1990. Gravity and deep seismic reflection profiles across the North Sea rifts. In: Blundell, D.J., Gibbs, A. (Eds.), Tectonic Evolution of the North Sea rifts. Oxford University Press, London, pp. 82–101.
Hospers, J., Ediriweera, K.W., 1988. Mapping of the top of the crystalline crust in the Viking Graben Area, North Sea. In: Kristoffersen, Y. (Ed.), Progress of the Studies of the Lithosphere in Norway: Norges Geologiske Undersøkelse, Special Publication, 3, pp. 21–28.
Hunt, C., Moskowitz, B.M., Banerje, S.K., 1995. Magnetic properties of rocks and minerals, in: Rock Physics and Phase Relations, A Handbook of Physical Constants. AGU Reference Shelf 3, 189–204.
Hurich, C.A., Kristoffersen, Y., 1988. Deep structure of the Caledonide orogen in southern Norway: new evidence from marine seismic reflection profiling. In: Kristoffersen, Y. (Ed.), Progress in Studies of the Lithosphere in Norway: Norges Geologiske Undersøkelse, Special Publication, 3, pp. 96–101.
Hyndman, R.D., Peacock, S.M., 2003. Serpentinization of the forearc mantle. Earth and Planetary Science Letters 212, 417–432.
Jamtveit, B., Austrheim, H., 2010. Metamorphism: the role of fluids. Elements 6, 153–158.
Keary, P., Vine, F.J., 1996. Global Tectonics, second ed. Blackwell Science, UK.
Kelley, D.S., Karson, J.A., Früh-Green, G., Yoerger, D.R., Shank, T.M., Butterfield, D.A., Hayes, J.M., Schrenk, M.O., Olson, E.J., Proskurowski, G., Jakuba, M., Bradley, A., Larson, B., Ludwig, K., Glickson, D., Buckman, K., Bradley, A.S., Brazelton, W.J., Roe, K., Elend, M.J., Delacour, A., Bernascone, S.M., Lilley, M.D., Baross, J.A., Summons, R. E., Sylva, S.P., 2005. A serpentinite-hosted ecosystem: the lost city hydrothermal field. Science 307 (5714), 1428–1434.
Kelso, P.R., Richler, C., Pariso, J.E., 1996. Rock magnetic properties, magnetic mineralogy and paleomagnetism of peridotites from site 895, Hess Deep. In: Mevel, C., Gillis, K. M., Allan, J.F., Meyer, P.S. (Eds.), Proceedings of the Ocean Drilling Program, Scientific results, 147.
Kido, Y., Fujioka, K., Machida, S., Sato, H., 2002. Present and fossil serpentine diapirs as sources of geophysical anomalies along forearc regions of Izu-Bonin Mariana and southwest Japan. Frontier Research on earth evolution 1, 341–344.
Kido, Y., Kido, M., Fujioka, K., 2004. Magnetic dipole anomalies as indicators of mantle wedge serpentinization. G3—Electronic Journal by AGU and Geochemical Society 5 (8), 1–12.
Klemperer, S.L., 1988. Crustal thinning and the nature of extension in the northern North Sea from deep seismic reflection profiling. Tectonics 7, 801–821.
Klemperer, S.L., Hurich, C.A., 1990. Lithospheric structure of the North Sea from deep seismic profiling. In: Blundell, D.J., Gibbs, A.D. (Eds.), Tectonic Evolution of the North Sea Rifts. Clarendon, Oxford, pp. 37–63.
Kostenko, O., Jamtveit, B., Austrheim, H., Pollok, K., Putnis, C., 2002. The mechanism of fluid infiltration in peridotites at Almkløvdalen, western Norway. Geofluids 2, 203–215.
Kubala, M., Bastow, M., Thompson, S., Scotchman, I., Oygard, K., 2003. Geothermal regime, petroleum generation and migration. In: Evans, D., Graham, C., Armour, A., Bathurst, P. (Eds.), The Millenium Atlas: Petroleum Geology of the Central and Northern North Sea: The Geological Society of London, pp. 285–315.
Kyrkjebø, R., Kjennerud, T., Gillmore, G.K., Faleide, J.I., Gabrielsen, R.H., 2001. Cretaceous–Tertiary palaeo-bathymetry in the northern North Sea; integration of palaeo-water depth estimates obtained by structural restoration and micropalaentological analysis. In: Martinsen, O. (Ed.), Sedimentary Environments Offshore Norway—Palaeozoic to Recent: Norwegian Petroleum Society Special Publication, 9, pp. 321–345.
Lampe, C., Person, M., 2002. Advective cooling within sedimentary rift basins—application to the Upper Rhinegraben (Germany). Marine and Petroleum Geology 19 (3), 361–375.
Lavier, L.L., Manatschal, G., 2006. A mechanism to thin the continental lithosphere at magma poor margins. Nature 440, 324–328.
Livermore, R.A., Smith, A.G., Briden, J.C., 1985. Paleomagnetic constraints on the distribution of continents in Late Silurian and early Devonian. Philosophical Transactions of the Royal Society of London 309, 29–56.
Lundin, E.R., Doré, A.G., 2011. Hyperextension, serpentinization, and weakening: a new paradigm for rifted margin compressional deformation. Geology 39, 347–350.
McKenzie, D.P., 1978. Some remarks on the development of sedimentary basins. Earth and Planetary Science Letters 40, 25–32.
McKenzie, D.P., Bickle, M.J., 1988. The volume and composition of melt generated by extension of the lithosphere. Journal of Petrology 29, 11–22.
Meert, J.G., Torsvik, T.H., 2003. The making and unmaking of a supercontinent: Rodinia revisited. Tectonophysics 375, 261–288.
Miller, J.A., Christensen, N.I., 1997. Seismic velocities of lower crustal and upper mantle rocks from the slow-spreading Mid-Atlantic ridge, south of the Kane Transform Zone (MARK). In: Karson, J.A., Cannat, M., Miller, D.J., Elthon, D. (Eds.), Proceedings of the Ocean Drilling Program, Scientific Results, 153, pp. 437–454.
Moore, D.E., Lockner, D.A., 2008. Talc friction in the temperature range 25°–400 °C: relevance for fault-zone weakening. Tectonophysics 449, 120–132.
Mørk, M.B.E., McEnroe, S., Olesen, O., 2002. Magnetic susceptibility of Mesozoic and Cenozoic sediments off Mid Norway and the role of siderite: implications for interpretation of high-resolution aeromagnetic anomalies. Marine and Petroleum Geology 19 (9), 1115–1126.
Mottle, M.J., 2009. Highest pH? Geochemical Society Online Publication: Geochemical News, gn141 (Oct09).
Nordgulen, Ø., Andresen, A., 2008. The Precambrian. In: Ramberg, I.B., Bryhni, I., Nøttvedt, A., Rangnes, K. (Eds.), The Making of a Land; Geology of Norway. The Norwegian Geological association, Trondheim.
Odinsen, T., Reemst, P., Van Der Beek, P., Faleide, J.I., Gabrielsen, R.H., 2000. Permo-Triassic and Jurassic extension in the northern North Sea: results from tectonostratigraphic forward modeling. Geological Society, London, Special Publications 167, 83–103.
Olesen, O., Balling, N., Barrère, C., Breiner, N., Davidsen, B., Ebbing, J., Elvebakk, H., Gernigon, L., Koziel, J., Lutro, O., Midttømme, K., Nordgulen, Ø., Olsen, L., Osmundsen, P.T., Pascal, C., Ramstad, R.K., Rønning, J.S., Skilbrei, J.R., Slagstad, T., Wissing, B., 2007. KONTIKI Final Report, Continental Crust and Heat Generation In 3D. Geological Survey of Norway Report No. 2007.042. 438 pp.

Olesen, O., Brönner, M., Ebbing, J., Gellein, J., Gernigon, L., Koziel, J., Lauritsen, T., Myklebust, R., Pascal, C., Sand, M., Solheim, D., Usov, S., 559–586, 2010. New aeromagnetic and gravity compilations from Norway and adjacent areas: methods and applications. In: Vining, B.A., Pickering, S.C. (Eds.), Petroleum Geology: From Mature Basins to New Frontiers—Proceedings of the 7th Petroleum Geology Conference, pp. 559–586.

Osland, R., 1997. Modeling of variations in Norwegian olivine deposits. Ph.D. thesis, NTNU, Trondheim, Norway, 190 pp.

Oufi, O., Cannat, M., Horen, H., 2002. Magnetic properties of variably serpentinized abyssal peridotites. Journal of Geophysical Research 107 (B5) 19 pp..

Pascal, C., Olesen, O., 2009. Are the Norwegian mountains compensated by a mantle thermal anomaly at depth? Tectonophysics 475, 160–168.

Perez-Gussinye, M., Reston, T.J., 2001. Rheological evolution during extension at passive non-volcanic margins: onset of serpentinization and development of detachments to continental breakup. Journal of Geophysical Research 106, 3961–3975.

Pharaoh, T.C., 1999. Palaeozoic terranes and their lithospheric boundaries within the Trans-European Suture Zone (TESZ): a review. Tectonophysics 314, 17–41.

Pickering, K.T., Smith, A.G., 1995. Arcs and backarc basins in the early Palaeozoic Iapetus Ocean. The Island Arc 4, 1–67.

Puchkov, V.N., 2009. The diachronous (step-wise) arc-continent collision in the Urals. Tectonophysics 479, 175–184.

Ramberg, I.B., Bryhni, I., Nøttvedt, A., Rangnes, K., 2008. The Making of a Land; Geology of Norway. The Norwegian Geological association, Trondheim.

Rasmussen, R., Pedersen, L.B., 1979. End corrections in potential field modeling. Geophysical Prospecting 27, 749–770.

Rey, P., Burg, J.-P., Casey, M., 1997. The Scandinavian Caledonides and their relationship to the Variscan belt. In: Burg, J.P., Ford, M. (Eds.), Orogeny Through Time: Spec. Publ. Geol. Soc. of London, 122, pp. 179–200.

Roberts, A.M., Yielding, G., Kusznir, N.J., Walker, I., Dornlopez, D., 1995. Quantitative analysis of Triassic extension in the northern North Sea. Journal of the Geological Society of London 152, 15–26.

Rohr, T.S., Corfu, F., Austrheim, H., Andersen, T.B., 2004. Sveconorwegian U–Pb zircon and monazite ages of granulite facies rocks, Hisarøya, Gulen, Western Gneiss Region, Norway. Norwegian Journal of Geology 84 (4), 251–256.

Seibold, U., Schilling, F.R., 2003. Heat transport in serpentinites. Tectonophysics 370, 147–162.

Shive, P.N., Frost, B.R., Peretti, A., 1988. The magnetic properties of metaperidotitic rocks as a function of metamorphic grade: implications for crustal magnetic anomalies. Journal of Geophysical Research 93 (B12), 187–195.

Slagstad, T., Barrére, C., Davidsen, B., Ramstad, R.K., 2008. Petrophysical and thermal properties of pre-Devonian basement rocks on the Norwegian continental margin. Geological Survey of Norway Bulletin 448, 1–6.

Slagstad, T., Davidsen, B., Daly, J.S., 2011. Age and composition of crystalline basement rocks on the Norwegian continental margin; offshore extension and continuity of the Caledonian–Appalachian orogenic belt. Journal of the Geological Society 168, 1–19.

Smethurst, M., 2000. Land-offshore links in western Norway and the northern North Sea. Journal of the Geological Society 157, 769–781.

Soper, N.J., England, R.W., Snyder, D.B., Ryan, P.D., 1992. The Iapetus suture zone in England, Scotland and eastern Ireland: a reconciliation of geological and deep seismic data. Journal of the Geological Society 149, 697–700.

Spengler, D., van Roermund, H.L.M., Drury, M.R., Ottolini, L., Mason, P.R.D., Davies, G.R., 2006. Deep origin and hot melting of an Archaean orogenic peridotite massif in Norway. Nature 440, 913–917.

Talwani, M., Worzel, J.L., Landisman, M., 1959. Rapid gravity computations for two-dimensional bodies with application to the Mendocino Submarine Fracture Zone. Journal of Geophysical Research 64, 49–61.

Thybo, H., Nielsen, C.A., 2009. Magma-compensated crustal thinning in continental rift zones. Nature 457, 873–876.

Tucker, R.D., Robinson, P., Solli, A., Gee, D.G., Thorsnes, T., Krogh, T.E., Nordgulen, Ø., Bickford, M.E., 2004. Thrusting and extension in the Scandian hinterland, Norway: new U–Pb ages and tectonostratigraphic evidence. American Journal of Science 304, 477–532.

Verhoef, J., Roest, W.R., Macnab, R., Arkani-Hamed, J., 1996. Magnetic anomalies of the Artic and Atlantic Oceans and adjacent land areas. GSC Open File 3125, Parts a and b (CD-Rom and project report). Geological Survey of Canada.

Warner, M., 2004. Free water and seismic reflectivity in the lower continental crust. Journal of Geophysics and Engineering 1, 88–101.

Warren, C.J., Beaumont, C., Jamieson, R.A., 2008. Modeling tectonic styles and the ultra-high pressure (UHP) rock exhumation during the transition from oceanic subduction to continental collision. Earth and Planetary Science letters 267, 129–145.

Wernicke, B., 1985. Uniform-sense normal simple shear of the continental lithosphere. Canadian Journal of Earth Sciences 22, 108–125.

Winter, J.D., 2009. Principles of Igneous and Metamorphic Petrology. Prentice Hall.

Zanella, E., Coward, M.P., 2003. Structural Framework. In: Evans, D., Graham, C., Armour, A., Bathurst, P. (Eds.), The Millennium Atlas: Petroleum Geology of the Central and Northern North Sea. The Geological Society of London, London, pp. 4–17.